Nuclear Engineering and Technology 52 (2020) 647–653

Contents lists available at ScienceDirect

Nuclear Engineering and Technology

journal homepage: www.elsevier.com/locate/net

Original Article

High alloyed new stainless steel shielding material for gamma and fast neutron radiation

Bünyamin Aygün

Agri Ibrahim Cecen University, Department of Electronics and Automation, Vocational School, Agri, Turkey

ARTICLE INFO

Article history:
Received 31 May 2019
Received in revised form
8 August 2019
Accepted 20 August 2019
Available online 22 August 2019

Keywords:
Stainless steel
Alloy
Neutron shielding
Geant4
Gamma

ABSTRACT

Stainless steel is used commonly in nuclear applications for shielding radiation, so in this study, three different types of new stainless steel samples were designed and developed. New stainless steel compound ratios were determined by using Monte Carlo Simulation program Geant 4 code. In the sample production, iron (Fe), nickel (Ni), chromium (Cr), silicium (Si), sulphur (S), carbon (C), molybdenum (Mo), manganese (Mn), wolfram (W), rhenium (Re), titanium (Ti) and vanadium (V), powder materials were used with powder metallurgy method. Total macroscopic cross sections, mean free path and transmission number were calculated for the fast neutron radiation shielding by using (Geant 4) code. In addition to neutron shielding, the gamma absorption parameters such as mass attenuation coefficients (MACs) and half value layer (HVL) were calculated using Win-XCOM software. Sulfuric acid abrasion and compressive strength tests were carried out and all samples showed good resistance to acid wear and pressure force. The neutron equivalent dose was measured using an average 4.5 MeV energy fast neutron source. Results were compared to 316LN type stainless steel, which commonly used in shielding radiation. New stainless steel samples were found to absorb neutron better than 316LN stainless steel at both low and high temperatures.

1. Introduction

Neutron and gamma radiation are used in nuclear plants and in many of applications such as high-energy physics, radio diagnosis and therapy, material analysis and radiography [1]. For this reason, the use of radiation is increasing each day in technology, medicine and military.

In addition, to population growth, the need for energy is also increasing, which results in building new nuclear power plants. During these applications, radiation may leak into the environment and cause significant damage to living tissues and organs. For instance radiation absorption in high ratio may cause serious effects such as radiation burns, cell and DNA damage, hereditary nervous system damage, etc. Furthermore, low ratio of radiation absorption for a long time may also cause many types of cancer [2,3]. Hence, for the efficient use of radiation, appropriate protection must be provided in accordance with the radiation type. For example, to reduce the negative effects of neutron radiation some materials are used such as polymers, heavy concretes, paraffin etc. To absorb gamma radiations, the materials with a bigger atomic number and higher density are used. For example, over 25 different metal alloys are used within the primary and secondary systems in a modern light water reactor. These materials have low strength at high temperature, therefore, stainless steels, particularly 316LN stainless steel are used for radiation shielding in a variety of applications, most commonly in nuclear reactors as structural shielding materials at reactor core heat transport system and in neutron moderator system. Shielding material very complex used in a nuclear power plant may degrade due to the various environmental conditions, radiation effect and stress [4]. In fact, the 316LN stainless steel's radiation absorption ability is low in both fast neutron and gamma. Therefore, the researches for new steel and alloy with high gamma and neutron shielding ability are ongoing. For example, in a study, by adding some elements into stainless steel have increased the ability of its radiation absorption. Austenitic stainless steels have been used to shield radiation at the magnetic fusion nuclear reactors [5]. The composition of this steel was modified with nickel and manganese for a long time use proved [6]. The chromium element in the alloy is important in terms of oxidation resistance and high temperature corrosion. So materials such as corrosion-resistant steels, stainless steels,

E-mail address: baygun@agri.edu.tr.

https://doi.org/10.1016/j.net.2019.08.017

Ni–Cr–Fe alloys and super alloys, Ni–Cr–Mn–W–Ti, etc.; Contain sufficient amount of chromium elements [7]. Fe–Cr–Mn stainless steel alloys have been produced for radiation shielding in the fusion reactors and it compared with typical Fe–Cr–Ni austenitic stainless steels [8]. The shielding property of some materials can be determined in terms of various parameters such as total macroscopic cross sections, mean free path, transmission, capture for neutron, mass attenuation coefficient, linear attenuation coefficient, half value thickness, effective atomic number, etc. for gamma radiation [9]. For example, for the gamma radiation shielding parameters such as mass attenuation coefficients, effective atomic numbers, half thickness value and mean free path of some type carbon and stainless-steel samples were found by using Monte Carlo simulation Geant4 and MCNP codes [10]. The neutron radiation absorption cross section and attenuation coefficients of the boron added type KTA-304 stainless steels were compared by the Monte Carlo simulation method with the conventional type SUS304 stainless steel shield parameter, it was reported that boron added steel had better property such as temperature, chemical corrosion resistance and neutron stopping [11]. Nickel added stainless steel alloys are corrosive and high temperature resistant so it is used in nuclear plants, in chemical, petrochemical industries; moreover, nickel-based super alloys and steels can be produced by adding refractory elements such as nickel, cobalt, chromium, aluminium, titanium [12]. In another study, gamma and neutron absorbed dose rates have found for metal alloys such as CS-516, SS-403, SS-410, SS-316, SS-316L, SS-304L, Incoloy-600, Monel-400 and Cupro-Nickel [13]. In this presented study, three different new stainless steel with the ability of keeping neutron and gamma radiation, including high rates of nickel, were produced and researched.

2. Materials and methods

2.1. Monte Carlo simulation codes Geant4

The Geant4 simulation toolkit code depends on the targeted material type and geometry with various particle and photon energies. The experimental setup of the simulation lets us to predict events that might occur between radiation and the targeted material. It is used in applications in nuclear and high energy physics, in the particle accelerator, materials research and medical physics [14]. Comprehensive information can be seen at www.Geant4.org.

2.2. Theoretical basis

The total macroscopic cross section (cm^{-1}) most important parameter for shielding neutron particle and this value theoretically were determined for 4.5 MeV energy fast neutron by using Monte Carlo simulation Geant4 code. The results are given in Table 4. While Fig. 3 shows the neutron irradiation setup. The cross section is used to express the possibility of reactions between neutrons and the target material in nuclear and particle physics [15]. How a neutron or particle can interact with the target material classified by the cross-section. The probability of a neutron's reaction with the light particle or nucleus by microscopic cross-section (σ) and the probability of interaction with the heavy materials such as concrete is determined by macroscopic cross section. Neutrons can interact like scattering, absorption, capture, fission, etc. with target material, so cross section is expressed in the form of total macroscopic cross section ($\sum$) and it is calculated as follows.

$$\sum = N\sigma \tag{1}$$

Here σ has unit refers to microscopic cross-section with m^2

$$N = \frac{\rho}{A} N_A \tag{2}$$

N; atomic density of the target material, ρ; density of the target material, NA; the number of Avogadro.

$$\Sigma\, Total = \Sigma\, scattering + \Sigma\, absorption + \Sigma\, capture + \Sigma\, fission + \ldots (3)$$

Materials with large total cross section are good neutron moderators, which means high possibility of interaction with the materials [16].

The mean free path λ is defined as the average distance of a neutron particle's travel between two collisions with target material. The probability of collision at a distance *dx* taken by a neutron in the material is calculated by the following equation.

$$p(x)dx = \sum_t dx.e^{-\Sigma_t}.x = \sum_t .e^{-\Sigma_t}.x\, dx \tag{4}$$

The distance (x) that neutrons can take in the material without any interaction is determined by means of mean free (λ).

$$\lambda = \int_0^\infty x.p(x)dx = \sum t \int_0^\infty e^{-\sum t} dx = \frac{1}{\sum t} \tag{5}$$

Σ^t; represents the possibility of a neutron interacting per length [17].

Neutron transmission number of incoming and passing neutrons on the material is expressed by transmission. 100000 fast neutrons were sent to each material and neutron numbers passing through the materials were determined by using Monte Carlo simulation the Geant4 code.

2.3. Sample preparation

To determine radiation interactions of nickel and of other components in new stainless steel alloys, a series of many simulations were carried out. Much preliminary work was done, calculated the materials of iron, tungsten, chromium and other compound ratios required to produce the desired new stainless steel alloys sample with Monte Carlo simulation code. In the production of samples and the Nano-sizes powder form materials, iron, nickel, chromium, silicon, sulphur, carbon, molybdenum, manganese, titanium, tungsten, vanadium, rhenium and powder metallurgy method were used. Materials were mixed for 15 min and formed homogeneous mixture was heated at 350 °C and then pelletized at 600 MPa pressure. The pellet formed samples were annealed at 1300 °C for 3 h, then the annealed stainless steel samples were hardened by the faster cooling process. The chemical compositions of the produced new stainless steel samples are shown in Table 1 and a picture of the samples is shown in Fig. 1.

In order to determine the corrosion resistance of the new stainless steel samples, nominally 95–98% sulfuric acid (H_2SO_4) were used which the most strongly abrasion for alloys and steels. The tests were carried out using conventional weight and thickness loss method. Each sample was kept sulfuric acid bath for 96 h [18]. Then, measurement of weight and thickness loss of the samples was done. The detailed results are shown in Table 2.

To determine the maximum mechanical strength (yield stress) of the new high alloys, stainless steel samples having 4 mm thickness and 20 mm diameter, Specac brand hydraulic pressure machine was used.

Table 1
Chemical composition ratios and density of producing stainless steel alloy (SSA) (%).

Elements (%)	SSA1 ($\rho = 9.04$ g/cm^3)	SSA2 ($\rho = 9.85$ g/cm^3)	SSA3 ($\rho = 10.45$ g/cm^3)
Ni	38	22	30
Cr	10	18	15
Mn	2	2	1
C	0.5	1	0.5
Mo	1	–	1
W	15	18	20
Si	1	–	–
Ti	3	2	–
Fe	29.5	35.975	31.47
V	–	1	0.015
S	–	–	0.015
Re	–	0.025	1

Stainless Steels Alloy (SSA).

Fig. 1. Produced stainless steels, alloy samples.

Table 2
Abrasion resistance results of the new high alloys stainless steel samples.

Sample	Wight of Sample (g)		Average loss (g)	Thickness (mm)		Average loss (mm)
Code	Before	After		Before	After	
SSA1	10	9.997	0.003	2	1.970	0.03
SSA2	10	9.998	0.002	2	1.981	0.019
SSA3	10	9.999	0.001	2	1.979	0.001

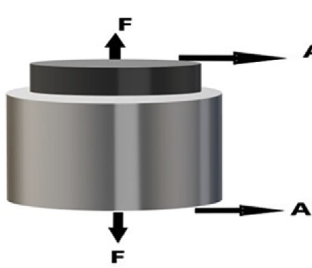

Fig. 2. Effect of applied force on surface area.

Diameter change must be found with the applied force of material, to calculate the yield strength. So in the current study, the diameter values before and after the force application were determined, then the yield stress values were calculated by using following formula [19].

$$\sigma = F/S \tag{6}$$

As shown in Fig. 2 where, F is the force at yield, S is the [original cross section area– sectional area (A-A_0)], σ is the yield stress, A is the cross-sectional area after of force applied. A_0 is the area before force applied. The obtained results are given in Table 3. All new high alloy stainless steel samples were weldability tested by using the arc welding method.

Table 3
Mechanical strength test results of the new high alloys stainless steel samples.

Sample	Diameter of Sample (mm)		Fracture load (1000 kg)	Yield Stress	
	Before	After		MPa	kgf/mm^2
SSA1	20	26.4	14.7	1120.8	114.29
SSA2	20	24.9	15.3	1990.1	202.94
SSA3	20	23.1	15.8	5135.6	523.69

2.4. Experimental dose measurements

For neutron absorbed dose rate measurement ^{241}Am/Be fast neutron source which emits 2–11 MeV neutron particles, Canberra NP100B–BF3 gaseous neutron detector and Canberra ADM606 series of digital rate meter were used. Experimental neutron dose rate measurement system is shown in Fig. 3.

3. Results and discussion

In this study, three different new types of high-alloyed stainless steel samples are designed and produced; the chemical compositions are shown in Table 1 which include three main components of steel with nickel content, 22–38 wt%, chromium content, 10–18 wt %, tungsten content 15–20 wt%. This new type high alloys stainless steel content nickel 22–38 wt %, and chromium 10–18%. So this new type high alloys stainless steel closer in the steels of the austenitic class. It has been seen that by adding nickel, chromium, and tungsten into the steel's structure has increased heat-resistance and radiation shielding properties. 5 tons under load mechanical strength, sulfuric acid (H_2SO_4) bath for 96 h, leaving in chemical abrasion and weldability tests were performed. Test results showed desired standard values.

3.1. Physical and mechanical properties

Products of the new high alloys stainless steel samples some physical and basic mechanical properties such as sulfuric acid corrosion and high temperature resistant, pressure strength, weldability were determined. Ni, Cr, W, elements were high rate added to the composition of the new steel samples thus the high temperature, corrosion, pressure strength and radiation shielding properties of the steel were increased. Acid abrasion tested and the results are given in Table 2.

As shown in Table 2 at the wear oxidation such as weight and thickness loss no significant changes were determined. The results

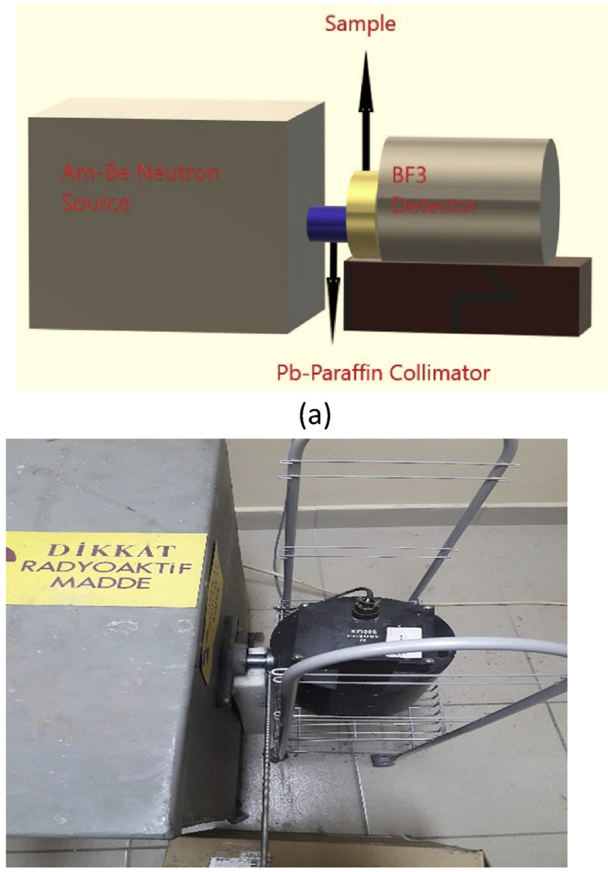

Fig. 3. (**a-b**). Neutron equivalent dose rate measurement system.

showed that the new stainless steel samples have high acid abrasion resistant.

Stainless steels can crack after the welding process and all type stainless steels have a potential risk to cracking during the and after welding process [20,21]. As a result of this test, all new high alloy stainless steel samples have been identified. New stainless steel samples have not been cracked after welding.

The yield point and yield strength resistance that indicates the limit of the beginning of a material plastic behavior.

Yield strength is an important property which has a key role in resistance of a material against plastic deformation [22].

As shown in Table 3, mechanical stress experimental results were determined.

Obtained this yield stress values are compatible with commercial stainless steel standards.

3.2. Neutron shielding parameters

The Total Macroscopic Cross Section, Mean free path and transmission number are important parameters for neutron shielding study. These parameters must be calculated to know of a material shielding character so in this study, these theoretically determined by using Monte Carlo Simulation Geant4 code and obtained results are shown in Table 4.

As shown in Table 4 neutron shielding parameters (Total Macroscopic Cross Section, Mean Free Path and Transmission number) were calculated of the new stainless steel samples and obtained results were compared with 316LN type stainless steel which is used at the shielding radiation applications commonly.

According to 316 LN stainless steel, new stainless steel samples have high Total macroscopic cross sections, low Mean Free Path and Transmission number. If a materials have short mean free paths it can be said that it has a good shielding neutron radiation ability.

The less the number of neutrons passing through the material, the higher the neutron absorption power of the material.

As shown in Fig. 4, it is founded that total Macroscopic Cross Sections values of new stainless steel samples bigger than reference sample 316LN type stainless steel. This is an indication that the new stainless steel samples are capable of high shielding.

3.3. Neutron radiation equivalent absorbed dose measurements

All samples were placed between neutron source and detector then 4.5 MeV energy fast neutron equivalent dose rate measurements were carried out. As shown in Table 5 and in Fig. 4 the results are compared with 316 LN stainless steel that are commonly used for shielding neutron particle and it has been observed that new stainless steel samples are better than reference sample 316LN. SSA3 sample better than other samples for radiation-shielding

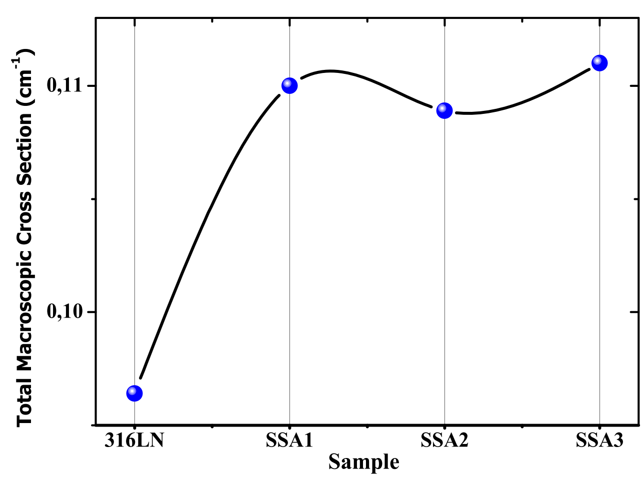

Fig. 4. Total macroscopic cross section (cm^{-1}).

Table 4
Total macroscopic cross sections, Mean free path, Transportation values of the samples 3 mm thick.

Sample code	Total macroscopic cross section (cm^{-1})	Mean Free Path (mm)	Transmission Number
316LN	0.0964	1.4886 ± 0.0868	90805
SSA1	0.1100	1.4818 ± 0.0848	89577
SSA2	0.1089	1.4882 ± 0.0871	89682
SSA3	0.1110	1.4840 ± 0.0862	89491

Table 5
Experimental equivalent absorbed dose results.

Sample	Equivalent Dose Rates Absorbed by Samples (μSv/h)	Absorbed Dose Rate (%)
Background	1,3824	–
316LN	0,4039	29%
SSA1	0,5261	38%
SSA2	0,5906	42%
SSA3	0,7021	50%

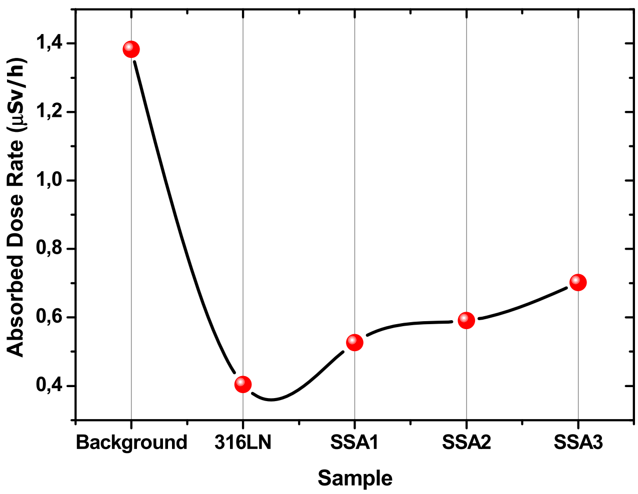

Fig. 5. Experimental neutron equivalent dose rate measurement results.

ability this is due to the fact that W concentration increased. From the results in Table 5 it can be seen that the 4.5 MeV neutron absorbed dose rate values of the new stainless steel alloy samples are higher than the 316LN type stainless steel taken as reference samples.

The absorbed equivalent dose rates of new stainless steel alloy samples and reference samples are compared in Fig. 4.

It can be seen from Fig. 5 that all samples show the highest absorption dose rate which better than 316 LN type stainless steel. It is an emphasize that all SSA1 samples possess highest shielding effectiveness than the 316 LN.

According to thickness (2-3-4-6-8-10-12-14-16-18- 20 mm) the amount of dose transmission passing was calculated by using Monte Carlo Simulation Geant4 code and as shown in Fig. 6 (a-b-c), obtained results are compared with reference sample 316LN. According to sample thickness neutron transmission change.

4.5 MeV energy 100000 fast neutron sent for each thickness and number of neutrons passing through the material was determined. It is clear from Fig. 6 (a-b-c) that as the thickness of all samples increases, the number of neutrons passed is significantly reduced almost more than percent fifty and this reduction is greater than 316 LN type stainless steel. It is evident that, the high alloy new stainless steel samples perfect shielding ability for fast neutron radiation.

3.3.1. Gamma radiation absorption calculations

The gamma radiation shielding ability of any material can be determined in terms of various parameters such as the mass attenuation coefficient, linear attenuation coefficient, mean free path, half value thickness, tenth value thickness, effective atomic number, effective electron number, etc. But important parameters are mass attenuation coefficient and half value thickness so these must be calculated to determine the character of the shielding materials to be used for gamma radiation.

Theoretical gamma-ray absorption parameters such as mass attenuation coefficient (MAC) and half value layer (HVL) of the samples are investigated by using the well-known Beer-Lambert law and Win-XCOM software [23,24]. The chemical compositions and densities of the samples are taken from Table 1. HVL is defined to be the thickness required to reduce the incident photon intensity by a factor of 1/2 [25,26]. Calculated MAC and HVL results are presented in Fig. 7 (a, b) in the continuous energy range of 0.1 MeV–100 GeV. In respect of MAC, the low energy region comparison is shown inset of Fig. 7 a. It is clearly seen that, the theoretical results are highly dependent on the chemical compositions of the samples and incident photon energies. In the low energy region, it may be seen that the MAC decreases rapidly with the increase in photon energy for all the samples. This result attributed to the dominance of the photoelectric absorption process. In this region the effective cross section is inversely proportional to the incident photon energy. Middle energy region (about 1 MeV) is dominated by another important process which is called Compton scattering. In this region the MAC values decrease slowly with the increasing energy. When Fig. 7a examined, it is clearly seen that the sample of SSA3 has the highest MAC values in all energies among the investigated samples. As this sample contains 96.47% of heavy metal, the MAC values are higher than the other samples. It means that, the sample of SSA3 has the highest effective atomic number and electron density. In addition to MAC values, the half value layer (HVL) of the samples are presented in the continuous energy range in Fig. 7b. The HVL is defined as the thickness required to halve the incoming radiation intensity. As it is seen from Fig. 6 the SSA3 sample has the smallest HVL in the investigated samples. Smallest HVL value means that higher radiation absorption ability [27].

4. Conclusion

The new stainless steel samples were produced at the three different content. Mass attenuation coefficients (cm^2/g) and half thickness values were calculated for six different energy gamma radiation. Equivalent absorbed dose rates were measured; total macroscopic cross section, mean free path and transmission number values were calculated for 4.5 MeV fast neutron particles. It was observed both the total cross section, mean free path, transmission number values and absorption power for fast neutron of the high-alloyed stainless steel samples were better than the standard 316LN type stainless steel. Neutron transmission number at 2 and 20 mm material thickness were calculated and the results were compared with 316 LN. It was determined that the decrease in the number of neutrons passing through all samples was very good compared to 316 LN due to thickness increase. Acid abrasion and mechanical strength were tested. Experimental studies showed that all samples were highly resistant to acid wear. All products were found to be able to weld according to the standards. The observed radiation shielding ability and the good mechanical properties as well as the high heat resistant properties of the high alloy stainless steel alloys make them as candidate materials for nuclear apply systems. In

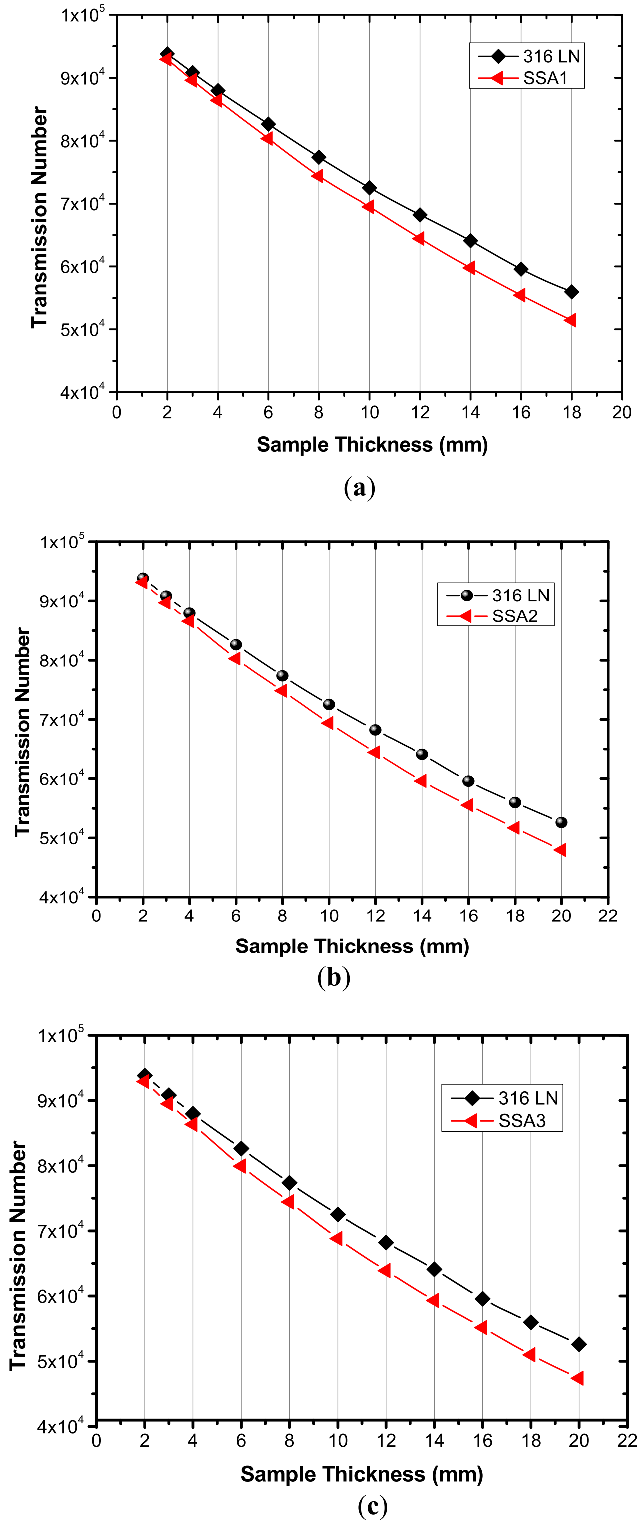

Fig. 6. (a-b-c). According to sample thickness neutron transmission change results.

general, products obtained in this study show the potential importance for radiation shielding applications and the stainless steel selection for nuclear reactor radiation safety.

Compliance with ethical standards

The author declare that anyone have no conflict of interest.

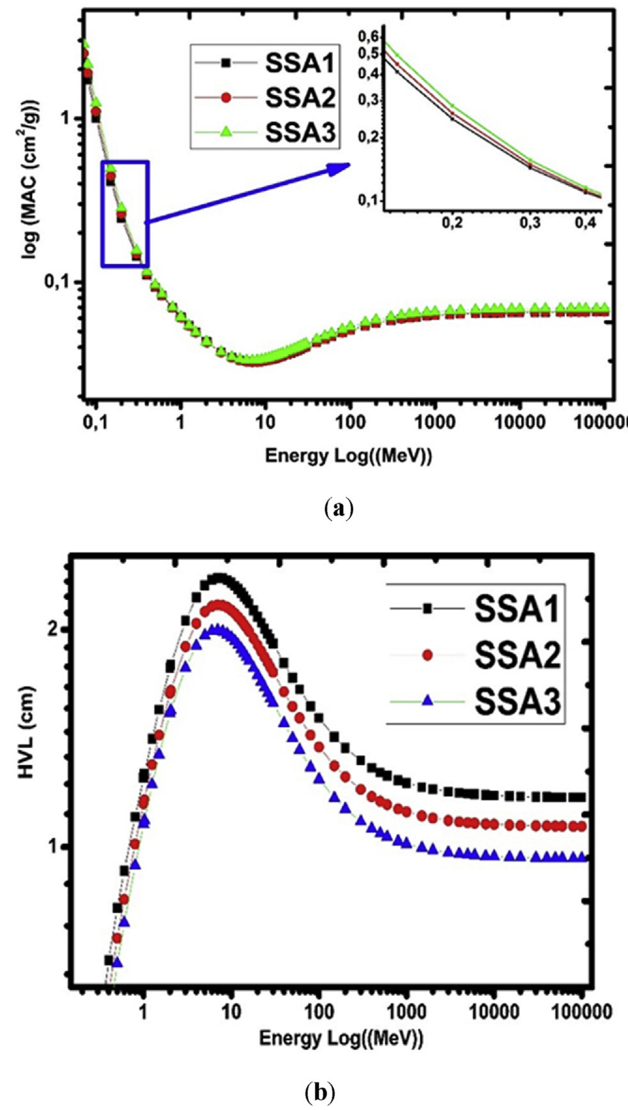

Fig. 7. Variations of radiation shielding parameters in continuous energy range a; MACs b; HVLs.

Acknowledgements

This work is financially supported by University of Atatürk with Grant No. 2016/FM7, FBA-2017-6312 and University of Agri Ibrahim Cecen with Grant no. MYO.18.001/Turkey.

Appendix A. Supplementary data

Supplementary data to this article can be found online at https://doi.org/10.1016/j.net.2019.08.017.

References

[1] U.S.NRC, United States Nuclear Regulatory Commission, 1997.
[2] 1 National Research Council, Health Risks from Exposure to Low Levels of Ionizing Radiation: BEIR VII Phase 2, The National Academies Press, Washington, DC, 2006, p. 7.
[3] R.E. Shore, et al., Implications of recent epidemiologic studies for the linear nonthreshold model and radiation protection, J. Radiol. Prot. 38 (2018) 1217–1233.
[4] V.P. Singh, N.M. Badiger, Gamma ray and neutron shielding properties of some alloy materials, Ann. Nucl. Energy 64 (2014) 301–310.
[5] Mukherjee, N.I. Jamnapara, Materials research and development opportunities

in fusion reactors, Proc. Indian Natl. Sci. Acad. 81 (4) (2015) 827−839.
[6] M. Kwon, Y.S. Bae, S. Cho, W. Choe, B.G. Hong, Y.S. Hwang, J.Y. Kim, K. Kim, Yaung-Soo Kim, Jong-Gu Kwak, Hyeon Gon Lee, Sangil Lee, Na Yong-Su, Byung-Hoon Oh, Yeong-Kook Oh, JiYeon Park, Hyung Lyeo Yang, In Keun Yu, Current status of nuclear fusion energy research in Korea, Nucl. Eng. Technol. 41 (2009) 4455−4476.
[7] W. Betteridge, J. Heslop, The Nimonic Alloys, and Other Nickel-Base High-Temperature Alloys, 1974, p. 29. New York.
[8] Fattah-Alhosseini, A.F. Shirsalimi, M. Yousefi, A. Abedi, Electrochemical behavior investigation of two low activation austenitic stainless steels in an acidic solution, J. Mater. Environ. Sci. 6 (2014) 1847−1853.
[9] T. Singh, P. Kaur, P.S. Singh, Thickness optimization of Sn−Pb alloys for experimentally measuring mass attenuation coefficients, Nucl. Energy Technol. 3 (2017) 1−5.
[10] D. Dawson, R. Fleck, A. Wadham, Radiation damage to materials, Approv. Issues Course Modul. 4 (1999) 228−230.
[11] W. Qianglin, Y. Bo, W. Yi, Y. Ting, L. Yibao, M-C simulation of slow neutron attenuation in boron- containing stainless steel, Nucl. Sci. Tech. 33 (5) (2010) 367−369.
[12] T. Yonezawa, Nickel alloys properties and characteristics, Ref. Modul. Mater. Sci. Mater. Eng. 2 (2016) 233−266.
[13] T. Dewen, Z. Shuliang, Y. Liang, Research on the preparation and shielding properties of W−Ni−Fe alloy material by liquid phase sintering, Powder Metall. 61 (1) (2018) 28−35.
[14] S. Agostinelli, et al., Geant4 simulation toolkit, Nucl. Instrum. Methods Phys. Res. 506 (2003) 250−303.
[15] F. Mughabghab, Neutron Cross-Sections, Neutron Resonance Parameters and Thermal Cross-Sections, vol. 4, Academic Press, 1984, pp. 61−100.
[16] V. McLane, C.L. Dunford, P.F. Rose, Neutron Cross Sections. 2, Neutron Cross Section Curves, N. P., Web, United States, 1988.
[17] P. Rinard, Neutron Interactions with Matter Passive Nondestructive Assay of Nuclear Materials, 1991.
[18] The International Nickel Company, inc, The Corrosion Resistance of Nickel-Containing Alloys in Sulfuric Acid, 1983.
[19] G.E. Dieter, Mechanical Metallurgy, third ed., McGraw Hill International Edition, New York (USA), 2014.
[20] V. Mclane, L. Charles, P. Dunford, F. Rose, Neutron Cross Sections, 1988, ISBN 978-0-12-484220-5.
[21] Ramesh Singh, Applied Welding Engineering, second ed., 2016, 978-0-12-8041, 76-5.
[22] William D. Callister Jr., G. David, Rethwisch Materials Science and Engineering an Introduction, ninth ed., 2004.
[23] M.J. Berger, J.H. Hubbell, XCOM Photon Cross Sections Database, Web Version 1.2, National Institute of Standard Sand Technology, Gaithersburg, MD 20899, USA, 1987 available at: http://physics.nist.gov/xcom. Originally published as NBSIR 87-3597 “XCOM:Photon Cross Sections on a Personal Computer.
[24] V.P. Singh, N.M. Badiger, N. Chanthima, J. Kaewkhao, Evaluation of gamma-ray exposure buildup factors and neutron shielding for bismuth boro silicate glasses, Radiat. Phys. Chem. 98 (2014) 14−21.
[25] M.I. Sayyed, F. Akman, V. Turan, A. Araz, Evaluation of radiation absorption capacity of some soil samples, Radiochim. Acta 107 (1) (2019) 83−93.
[26] M.I. Sayyed, Half value layer, mean free path and exposure buildup factor for tellurite glasses with different oxide compositions, J. Alloy. Comp. 695 (25) (2017) 3191−3197.
[27] K.O. Ott, W.A. Bezella, Introductory Nuclear Reactor Statics, Revised edition, American Nuclear Society, 1989, ISBN 0-894-48033-2.